Computers, Materials & Continua CMC, vol.65, no.2, pp.993-1014, 2020

Complementary Kalman Filter as a Baseline Vector Estimator for GPS-Based Attitude Determination

Dah-Jing Jwo[1, *]

Abstract: The Global Positioning System (GPS) offers the interferometer for attitude determination by processing the carrier phase observables. By using carrier phase observables, the relative positioning is obtained in centimeter level. GPS interferometry has been firstly used in precise static relative positioning, and thereafter in kinematic positioning. The carrier phase differential GPS based on interferometer principles can solve for the antenna baseline vector, defined as the vector between the antenna designated master and one of the slave antennas, connected to a rigid body. Determining the unknown baseline vectors between the antennas sits at the heart of GPS-based attitude determination. The conventional solution of the baseline vectors based on least-squares approach is inherently noisy, which results in the noisy attitude solutions. In this article, the complementary Kalman filter (CKF) is employed for solving the baseline vector in the attitude determination mechanism to improve the performance, where the receiver-satellite double differenced observable was utilized as the measurement. By using the carrier phase observables, the relative positioning is obtained in centimeter level. Employing the CKF provides several advantages, such as accuracy improvement, reliability enhancement, and real-time assurance. Simulation results based on the conventional method where the least-squares approach is involved, and the proposed method where the CKF is involved are compared and discussed.

Keywords: Global positioning system (GPS), attitude determination, complementary Kalman filter, baseline vector.

1 Introduction

The Global Positioning System (GPS) [Hofmann-Wellenhof, Lichtenegger and Wasle (2008); Parkinson, Spilker, Axelrad et al. (1996); Farrell and Barth (1999)] has traditionally been a position, velocity and time sensor using the code observable. Code and carrier phase observables are two common types of observables that can be extracted from the GPS signals. Due to its higher accuracy and precision compared to code observables, carrier phase observables can be used to achieve very high accuracy of

[1] Department of Communications, Navigation and Control Engineering, National Taiwan Ocean University, Keelung, 202-24, Taiwan.

[*] Corresponding Author: Dah-Jing Jwo. Email: djjwo@mail.ntou.edu.tw.

Received: 18 May 2020; Accepted: 03 June 2020.

CMC. doi:10.32604/cmc.2020.011592 www.techscience.com/journal/cmc

estimated position. Although carrier phase observable can be very accurately measured, it is not possible to use pure carrier phase observable for absolute positioning due to inherently contained integer cycle ambiguity. However, it provides relative positioning in centimeter level and has been widely applied to surveying, attitude determination [Boccia, Amendola and Di Massa (2008); Hauschild, Montenbruck and Langley (2020); Li, Nie, Chen et al. (2019); Li, Efatmaneshnik and Dempster (2012); Raskaliyev, Hosi Patel, Sobh et al. (2020); Ryzhkov (2019); Zhang, Zhao, Lin et al. (2020)] and precision approach and automatic landing.

If two antennas are attached to a vehicle, a baseline vector defined as a vector from the master antenna to one of the other antennas, sometimes referred to as the slave antennas, can be determined using relative positioning techniques. Very accurate relative position estimate in the centimetre level will be available if the integer ambiguities are properly resolved [Boccia, Amendola and Di Massa (2008); Hauschild, Montenbruck and Langley (2020); Li, Nie, Chen et al. (2019); Lu, Ma, Wu et al. (2019)]. The attitude of a vehicle can be precisely determined using GPS carrier phase measurements from more than two antennas attached to the vehicle. Attitude determination using GPS does not have the error accumulation, which happens in the inertial navigation system (INS) [Farrell and Barth (1999)]. There have been many efforts on real time GPS attitude determination problem. Real-time integer ambiguity resolution techniques and attitude determination are two main issues to be resolved for determining the vehicle attitude when applying GPS double-differenced carrier phase. Most of the investigation has been on the real-time integer ambiguity resolution techniques and attitude determination from the baseline vectors. GPS interferometry has been firstly used in precise static relative positioning, and thereafter in kinematic positioning. Some investigators utilized certain constraint factors such as baseline length or known geometry to resolve integer ambiguity in real-time manner.

The carrier phase differential GPS based on interferometer principles can solve for the antenna vector, shown as in Fig. 1 [Boccia, Amendola and Di Massa (2008)]. Define the baseline vector as the vector between the antenna designated master and one of the slave antennas. The approach is based on the difference in the GPS carrier phase received at two or more nearby antennas connected to a rigid body. By using carrier phase observables, the relative positioning is obtained in centimeter level provided that the integer ambiguity is resolved. In the beginning of 1990s, Van Grass et el. [Van Grass and Braasch (1991, 1992)] conducted research on the GPS to the field of aircraft attitude determination using carrier phase was developed. In their work, the receiver-satellite double differenced observable was employed.

Investigators have presented several Kalman filter [Brown and Hwang (1997); Gelb (1974); Lewis (1986); Grewal and Andrews (2001); Jwo and Cho (2007)] related applications in the fields of navigation, such as GPS receiver position and velocity determination [Brown and Hwang (1997); Farrell and Barth (1999)], inertial navigation alignment [Wang, Yang, Wu et al. (2019)], attitude determination [Li, Efatmaneshnik and Dempster (2012); Raskaliyev, Hosi Patel, Sobh et al. (2020)], and integrated navigation system design [Farrell and Barth (1999)]. Since the conventional baseline vector estimation in attitude determination algorithms based on the least-squares technique is inherently noisy, the Kalman filter incorporated into the GPS interferometer to improve

the solution is accessible.

Recent works on the issues of other filter related applications have been popular in various areas of expertises. Chen et al. [Chen, Wang, Liu et al. (2019)] presented the multiscale fast correlation filtering tracking algorithm based on a feature fusion model. A multiscale fast correlation filtering tracking algorithm based on the feature fusion model has been proposed. In the paper by Yin et al. [Yin, Shi, Sun et al. (2019)], an efficient privacy-preserving collaborative filtering algorithm was proposed based on differential privacy protection and time factor. In view of the long execution time and low execution efficiency of support vector machine in large-scale training samples, Chen et al. [Chen, Xiong, Xu et al. (2019)] proposed a paper where the online incremental and decremental learning algorithm was based on the variable support vector machine (VSVM).

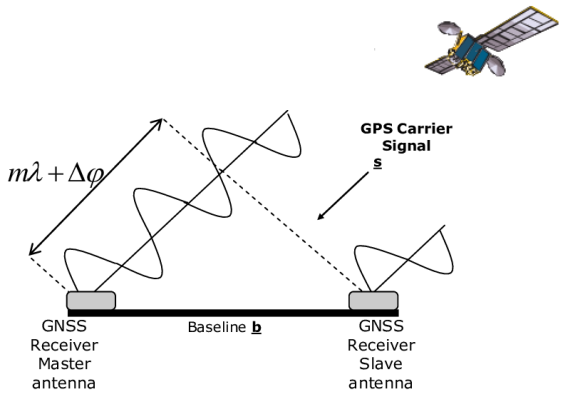

Figure 1: GPS interferometer

Simulation results of the attitude solutions by the conventional and proposed methods will be carried out and discussion will be presented. The remainder of this paper is organized as follows. In Section 2, preliminary background on the GPS carrier phase observation model is reviewed. The GPS-based attitude determination algorithms are introduced in Section 3. Section 4 presents the solutions of the baseline vector. In Section 5, simulation experiments are carried out to evaluate the performance on estimation error using the proposed method as compared to the conventional approach. Conclusions are given in Section 6.

2 GPS carrier phase observation model

The GPS pseudorange observable can be expressed as

$$\rho = r + c \cdot (dt - dT) + d_{ion} + d_{trop} + v_{\rho} \tag{1}$$

Carrier phase observables in GPS include sum of range, an unknown integer ambiguity and some ranging errors given by:

$$\Phi = r + c \cdot (dt - dT) + \lambda \cdot N - d_{ion} + d_{trop} + v_{\phi} \tag{2}$$

where the parameters involved in Eqs. (1) and (2) are defined as:

r : true range between a satellite and receiver;

c : speed of light;

dt : offset of the satellite clock from GPS time;

dT : offset of the receiver clock from GPS time;

d_{ion} : ionospheric error;

d_{trop} : tropospheric error;

λ : carrier phase wavelength;

N : carrier phase integer ambiguity;

v_ρ , v_ϕ : measurement noises of code and carrier phases.

Since the carrier phase observables contain measurement noise much smaller than that of code observables, mosteffort has been made to develop a technique to utilize the carrier phase observables. To utilize the carrier phase observables, the number of integer wavelengths contained in the phase difference needs to be determined, referred to as the 'integer ambiguity resolution'. By measuring the phase of the GPS carrier relative to the carrier phase at a reference site, single, double, and triple differences can be employed to determine the vector between the reference (designated master) and slave antennas and subsequently solve for the solutions of attitude determination problem. The receiver-satellite double differencing operator is defined as

$$\nabla\Delta(\bullet) = \Delta\nabla(\bullet) = \nabla(\bullet) - \Delta(\bullet)$$

where $\Delta(\bullet) = (\bullet)_1 - (\bullet)_2$ denotes the between receiver single differencing operator for receivers 1 and 2, and $\nabla(\bullet) = (\bullet)^i - (\bullet)^j$ denotes the between satellites single differencing operator for satellites *i* and *j*. It can be seen that the receiver-satellite double-differenced observable is essentially formed by a linear combination of four observations:

$$\nabla\Delta(\bullet)_{12}^{ij} = \{(\bullet)_2^j - (\bullet)_2^i\} - \{(\bullet)_1^j - (\bullet)_1^i\} \tag{3}$$

where the symbols '$\bullet$' can be either Φ , ρ , r , or N , and so on.

The between-receiver single-differenced observable greatly reduces the effects of errors associated with the satellites; while the between-satellite single-differenced observable is free from receiver clock errors. The receiver-satellite double-differenced observable eliminates or greatly reduces the satellite and receiver timing errors.

Adding the double-differenced noise term, v , and rewriting the observation equation between two receivers and two satellites by combining the carrier phase data from master (denoted as '1') and slave (denoted as '2') receivers to satellites i and j , we have

$$\nabla\Delta\Phi_{12}^{ij} = \nabla\Delta r_{12}^{ij} + \lambda\nabla\Delta N_{12}^{ij} - \nabla\Delta d_{ion} + \nabla\Delta d_{trop} + v \tag{4}$$

For a very short baseline, e.g., less than one meter between two antennas, most of the ionospheric and tropospheric errors become negligible. The resulting double-differenced phase equation when ignoring atmospheric, satellite ephemeris, and residual clock errors possesses the form

$$\nabla\Delta\Phi_{12}^{ij} = \nabla\Delta r_{12}^{ij} + \lambda\nabla\Delta N_{12}^{ij} + v \tag{5}$$

3 GPS-based attitude determination algorithms

The rotation angles that relate a coordinate system fixed in the body (body frame) to a coordinate system fixed in space are referred to as the attitudes. The purpose of attitude determination essentially includs calculation of the three Euler angles, namely roll, pitch, and yaw. The space coordinate system is typically defined to be a local level NED (north-east-down) frame, also referred to as the navigation frame. The baseline vector is defined as the vector between the antenna designated master and one of the slave antennas. The carrier phase differential GPS based on interferometer principles can solve for the antenna vector. The approach is based on the difference in the GPS carrier phase received at two or more nearby antennas connected to a rigid body. Multiple antenna vectors from an antenna array can be used to calculate the vehicle attitude. In general, three non-collinear antennas simultaneously receiving signals from two satellites are the minimum requirement to determine the three-dimensional attitude.

Referring to the configuration as in Fig. 2 [Van Grass and Braasch (1991, 1992)], when using the carrier phase signal from satellite i, the between-receiver single-differenced observable is a linear combination of two phase observables received by two antennas

$$\Delta\Phi^i = \Phi_1^i - \Phi_2^i = \mathbf{b}\cdot\mathbf{e}_i + \lambda\Delta N^i \tag{6}$$

Similarly, the single-differenced observable received for the same antennas from satellite j is

$$\Delta\Phi^j = \Phi_1^j - \Phi_2^j = \mathbf{b}\cdot\mathbf{e}_j + \lambda\Delta N^j \tag{7}$$

where $\mathbf{b}$ is the baseline vector formed by two antennas, and $\mathbf{e}$ represents the line-of-sight unit vector from antennas to satellites. The receiver-satellite double difference obtained by taking two independent single-differenced observables can be shown to be:

$$\nabla\Delta\Phi_{12}^{ij} = \Delta\Phi^i - \Delta\Phi^j = \mathbf{b}\cdot(\mathbf{e}_i - \mathbf{e}_j) + \lambda(\Delta N^i - \Delta N^j) = \mathbf{b}\cdot(\mathbf{e}_i - \mathbf{e}_j) + \lambda\nabla\Delta N_{12}^{ij} \tag{8}$$

Based on Eq. (8), signals received from n satellites by one GPS interferometer provide $n-1$ independent double differences

$$\begin{bmatrix} \nabla\Delta\Phi_{12}^{12} \\ \nabla\Delta\Phi_{12}^{13} \\ \vdots \\ \nabla\Delta\Phi_{12}^{1n} \end{bmatrix} = \begin{bmatrix} (\mathbf{e}_1 - \mathbf{e}_2)^{\mathrm{T}} \\ (\mathbf{e}_1 - \mathbf{e}_3)^{\mathrm{T}} \\ \vdots \\ (\mathbf{e}_1 - \mathbf{e}_n)^{\mathrm{T}} \end{bmatrix} \begin{bmatrix} b_x \\ b_y \\ b_z \end{bmatrix} + \begin{bmatrix} \lambda\nabla\Delta N_{12}^{12} \\ \lambda\nabla\Delta N_{12}^{13} \\ \vdots \\ \lambda\nabla\Delta N_{12}^{1n} \end{bmatrix} \tag{9}$$

When the integer ambiguity parameter ($\nabla\Delta N_{12}^{ij}$) is resolved, the range-based equivalent of Eq. (9) is depicted as follows:

$$\begin{bmatrix} \nabla\Delta r_{12}^{12} \\ \nabla\Delta r_{12}^{13} \\ \vdots \\ \nabla\Delta r_{12}^{1n} \end{bmatrix} = \begin{bmatrix} (\mathbf{e}_1 - \mathbf{e}_2)^{\mathrm{T}} \\ (\mathbf{e}_1 - \mathbf{e}_3)^{\mathrm{T}} \\ \vdots \\ (\mathbf{e}_1 - \mathbf{e}_n)^{\mathrm{T}} \end{bmatrix} \begin{bmatrix} b_x \\ b_y \\ b_z \end{bmatrix} = \begin{bmatrix} e_{12_x} & e_{12_y} & e_{12_z} \\ e_{13_x} & e_{13_y} & e_{13_z} \\ \vdots & \vdots & \vdots \\ e_{1n_x} & e_{1n_y} & e_{1n_z} \end{bmatrix} \begin{bmatrix} b_x \\ b_y \\ b_z \end{bmatrix} \tag{10}$$

which can be expressed in the matrix form

$$\nabla \Delta \mathbf{r} = \mathbf{G}\mathbf{b} \tag{11}$$

There have been various approaches proposed for the integer ambiguity resolution, including the ambiguity function, antenna exchange/swap, and baseline rotation methods [Li, Nie, Chen et al. (2019)]. The solution of the baseline vector $\mathbf{b} = [b_x \quad b_y \quad b_z]^{\mathrm{T}}$ is the approximate interferometer coordinates, which directly influence the performance of the GPS-based attitude determination. The accuracy of the attitude measurement depends on the baseline to noise ratio, and is also a function of antenna placement and GPS satellite geometry. There are several methods available for solving vehicle attitudes, typically including Euler angle method and quaternion method [Farrell and Barth (1999)].

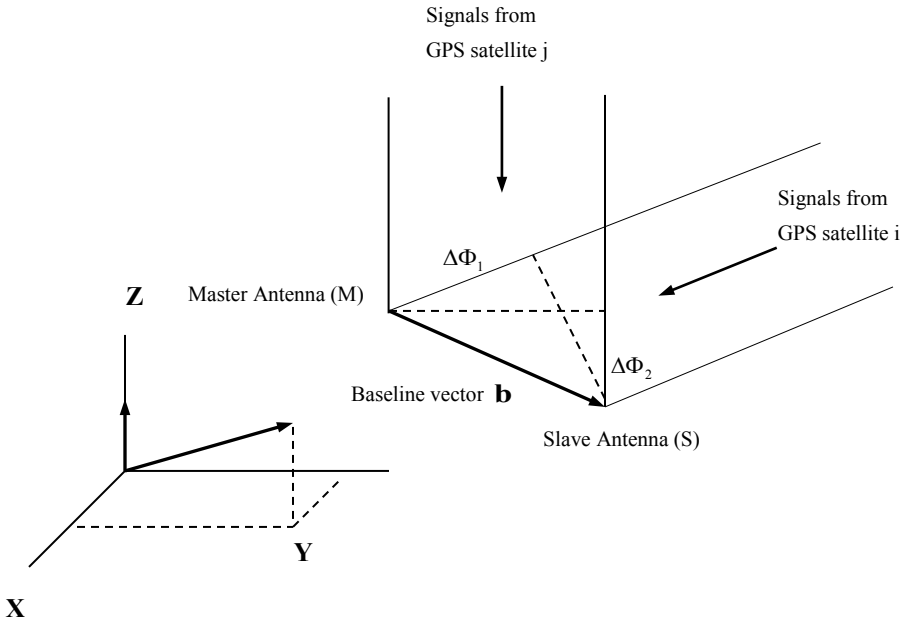

Figure 2: Receiver-satellite double differences and interferometer

Since the vehicle attitude is defined by the angles between the NED type of local frame and body frame, therefore, the rotation transformation matrix that relates the body and NED frames provides the information for finding the vehicle attitude [Farrell and Barth (1999); Van Grass and Braasch (1991, 1992); Kayton and Fried (1997)]

$$\mathbf{R}_{b2n} = \begin{bmatrix} C_\theta C_\psi & -C_\varphi S_\psi + S_\varphi S_\theta C_\psi & S_\varphi S_\psi + C_\varphi S_\theta C_\psi \\ C_\theta S_\psi & C_\varphi C_\psi + S_\varphi S_\theta S_\psi & -S_\varphi C_\psi + C_\varphi S_\theta S_\psi \\ -S_\theta & S_\varphi C_\theta & C_\varphi C_\theta \end{bmatrix} \tag{12}$$

where the subscripts n and b represent the local and body frames, respectively. Since $\mathbf{R}_{b2n}$ is an orthonormal matrix, its inverse can obtained through its transpose

$$\mathbf{R}_{n2b} = \mathbf{R}_{b2n}^{-1} = \mathbf{R}_{b2n}^{\mathrm{T}} \tag{13}$$

The vehicle attitude can be obtained through the calculation:

$$\theta = \sin^{-1}[-\mathbf{R}_{b2n}(3,1)]\,; \quad \varphi = \sin^{-1}\left(\frac{\mathbf{R}_{b2n}(3,2)}{\cos\theta}\right); \quad \psi = \sin^{-1}\left(\frac{\mathbf{R}_{b2n}(2,1)}{\cos\theta}\right) \tag{14}$$

In Eq. (12), the notations $S_{(\bullet)} \equiv \sin(\bullet)$ and $C_{(\bullet)} \equiv \cos(\bullet)$ are defined.

To perform the calculation of a platform attitude, the antennas should be set up as nonzero and are on the non-collinear vector. The configuration for the body-frame-mounted GPS antennas, and for two typical geometries based on two γ angles are shown as in Fig. 3. In this paper, we consider two body-frame-mounted baseline vectors: $\mathbf{b}_1 = \mathrm{S_A} - \mathrm{M}$ and $\mathbf{b}_2 = \mathrm{S_B} - \mathrm{M}$. The master antenna (M) position is located at $[0 \quad 0 \quad 0]^{\mathrm{T}}$ described in the body frame, while the two slave antennas $\mathrm{S_A}$ and $\mathrm{S_B}$ are at $[1 \quad 0 \quad 0]^{\mathrm{T}} d$ and $[\cos\gamma \quad \sin\gamma \quad 0]^{\mathrm{T}} d$, respectively, where d is the baseline length parameter used to adjust the length, and γ is the angles between two baseline vectors which is adjustable for design felxibility. For the case of $\gamma = \pi/3$, the two slave antennas $\mathrm{S_A}$ and $\mathrm{S_B}$ are located at $[1 \quad 0 \quad 0]^{\mathrm{T}} d$ and $[0.5 \quad 0.866 \quad 0]^{\mathrm{T}} d$, respectively; for the case of $\gamma = \pi/2$, the two slave antennas $\mathrm{S_A}$ and $\mathrm{S_B}$ are located at $[1 \quad 0 \quad 0]^{\mathrm{T}} d$ and $[0 \quad 1 \quad 0]^{\mathrm{T}} d$, respectively. Once the baseline vector is determined, estimation of the coordinate frame transformation $\hat{\mathbf{R}}_{b2n}$ can be achieved and subsequently the transformation matrix from body to local frame can be estimated through the following calculation [Farrell and Barth (1999)]

$$\hat{\mathbf{R}}_{b2n} = \hat{\mathbf{B}}^n (\mathbf{B}^b)^{-1} \tag{15}$$

where $\hat{\mathbf{B}}^n = [\hat{\mathbf{b}}_1^n, \hat{\mathbf{b}}_2^n, \hat{\mathbf{b}}_1^n \times \hat{\mathbf{b}}_2^n]$ and $\mathbf{B}^b = [\mathbf{b}_1^b, \mathbf{b}_2^b, \mathbf{b}_1^b \times \mathbf{b}_2^b]$.

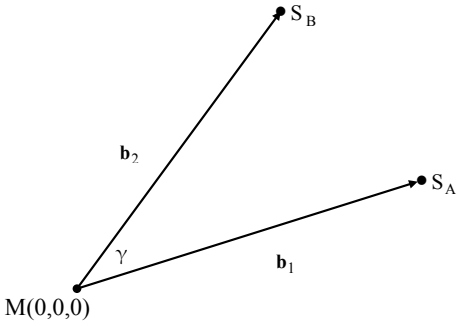

(a)

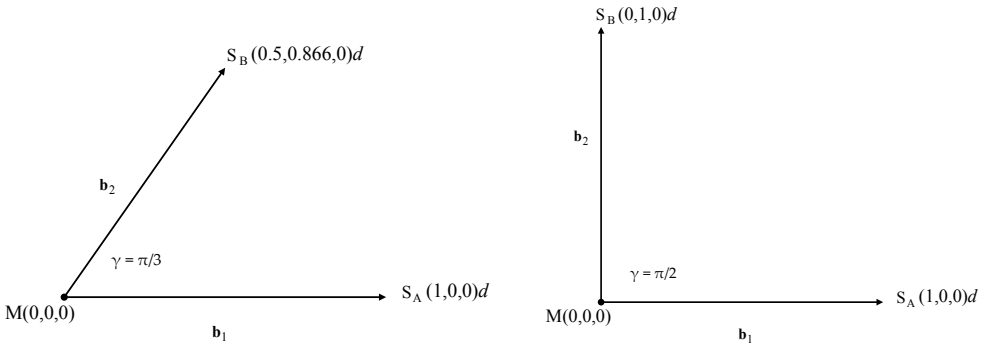

(b) (c)

Figure 3: Antenna differential position vector geometry: (a) configuration for body-frame-mounted GPS antennas; (b) $\gamma = \pi/3$; (c) $\gamma = \pi/2$

4 Solutions of the baseline vector for the GPS interferometer

Determination of the unknown baseline between the antennas sits at the heart of attitude determination. Eq. (11) interpretes the relation between the double-differenced carrier phase observables and the baseline vector. The solution is traditionally obtained based on the least-squares approach:

$$\mathbf{b} = (\mathbf{G}^{\mathrm{T}}\mathbf{G})^{-1}\mathbf{G}^{\mathrm{T}}\nabla\Delta\mathbf{r} \tag{16}$$

Since the result based on least-squares approach is noisy due to the inherently noisy double-differenced measurements, and therefore, the noisy estimation results for the baseline vector will result in noisy estimate of the platform/vehicle attitude. Utilization of the Kalman filter in the complementary configuration provides an approach for improving the accuracy.

4.1 The Kalman filter

The purpose of the Kalman filter [Brown and Hwang (1997); Gelb (1974); Lewis (1986); Grewal and Andrews (2001); Jwo and Cho (2007)] is to provide an optimal estimate of the system state vector. It has been successfully applied in the integrated GPS/INS navigation system design, stand-alone GPS receiver position/velocity determination, and the carrier-smoothed-code (CSC) processing. In this paper, the Kalman filter will be employed as the attitude estimator. Utilization of the Kalman filter enhances the accuracy and reliability of the attitude solution.

The Kalman filter algorithms are now briefly reviewed. Consider a dynamical system whose state is described by a linear, vector differential equation. The process model and measurement model are represented as

Process model: $\dot{\mathbf{x}} = \mathbf{F}\mathbf{x} + \mathbf{G}\mathbf{u}$ (17)

Measurement model: $\mathbf{z} = \mathbf{H}\mathbf{x} + \mathbf{v}$ (18)

It is assumed that $\mathbf{u}(t)$ and $\mathbf{v}(t)$ are white-noise processes with zero means and mutually independent:

$$E[\mathbf{u}(t)\mathbf{u}^{\mathrm{T}}(\tau)] = \mathbf{Q}\delta(t-\tau);\ E[\mathbf{v}(t)\mathbf{v}^{\mathrm{T}}(\tau)] = \mathbf{R}\delta(t-\tau);\ E[\mathbf{u}(t)\mathbf{v}^{\mathrm{T}}(\tau)] = 0 \tag{19}$$

where $\delta(t-\tau)$ is the Dirac delta function, $E[\cdot]$ represents expectation, and superscript "T" denotes matrix transpose. The discrete-time representation of Eq. (17) has the form

$$\mathbf{x}_{k+1} = \mathbf{\Phi}_{\mathrm{k}}\mathbf{x}_{\mathrm{k}} + \mathbf{w}_k \tag{20}$$

and the corresponding state transition matrix and process noise covariance matrix, respectively, are given by

$$\mathbf{\Phi}_{\mathrm{k}} = \pounds^{-1}[(s\mathbf{I}-\mathbf{F})^{-1}] = \mathbf{e}^{\mathbf{F}\Delta t} \tag{21}$$

$$\mathbf{Q}_k = \int_0^{\Delta t} \mathbf{e}^{\mathbf{F}\tau}\,\mathbf{G}\mathbf{Q}\mathbf{G}^{\mathrm{T}}\mathbf{e}^{\mathbf{F}^{\mathrm{T}}\tau}\,d\tau \tag{22}$$

where Δt is the step size. These two equations can also be approximated by the Taylor series expansion as follows:

$$\mathbf{\Phi}_k = \mathbf{I} + \mathbf{F}\Delta t + \frac{\mathbf{F}^2\Delta t^2}{2!} + \frac{\mathbf{F}^3\Delta t^3}{3!} + \cdots \tag{23}$$

$$\mathbf{Q}_k = \mathbf{G}\mathbf{Q}\mathbf{G}^{\mathrm{T}}\Delta t + \frac{(\mathbf{F}\mathbf{G}\mathbf{Q}\mathbf{G}^{\mathrm{T}} + \mathbf{G}\mathbf{Q}\mathbf{G}^{\mathrm{T}}\mathbf{F}^{\mathrm{T}})\Delta t^2}{2!} + \cdots \tag{24}$$

Numerical approach for evaluating $\mathbf{\Phi}_k$ and $\mathbf{Q}_k$ can be found in Brown et al. [Brown and Hwang (1997)] and will not be discussed here. The vectors $\mathbf{w}_k$ and $\mathbf{v}_k$ are white noise sequences with zero means and having zero cross-correlation with each other:

$$\mathbf{E}[\mathbf{w}_k\mathbf{w}_i^{\mathrm{T}}] = \mathbf{Q}_k\delta_{ik};\ \mathbf{E}[\mathbf{v}_k\mathbf{v}_i^{\mathrm{T}}] = \mathbf{R}_k\delta_{ik};\ \mathbf{E}[\mathbf{w}_k\mathbf{v}_i^{\mathrm{T}}] = \mathbf{0} \tag{25}$$

where $\mathbf{R}_k$ is the measurement noise covariance matrix. The symbol δ_{ik} stands for the Kronecker delta function:

$$\delta_{ik} = \begin{cases} 1, & i = k \\ 0, & i \neq k \end{cases}$$

Tab. 1 provides a list for the Kalman filter equations. More detailed discussion can be referred to Brown et al. [Brown and Hwang (1997)], and Gelb [Gelb (1974)].

Table 1: The Kalman filter equations

System Model	$\mathbf{x}_{k+1} = \mathbf{\Phi}_k\mathbf{x}_k + \mathbf{w}_k,\ \mathbf{w}_k \sim \mathrm{N}(\mathbf{0}, \mathbf{Q}_k)$
Measurement Model	$\mathbf{z}_k = \mathbf{H}_k\mathbf{x}_k + \mathbf{v}_k,\ \mathbf{v}_k \sim \mathrm{N}(\mathbf{0}, \mathbf{R}_k)$
Initial Conditions	$\mathrm{E}(\mathbf{x}_0) = \hat{\mathbf{x}}_0(-) = \mathbf{0};\ \mathrm{E}(\tilde{\mathbf{x}}_0\tilde{\mathbf{x}}_0^{\mathbf{T}}) = \mathbf{P}_0(-)$
Kalman Gain Matrix	$\mathbf{K}_k = \mathbf{P}_k(-)\mathbf{H}_k^{\mathbf{T}}[\mathbf{H}_k\mathbf{P}_k(-)\mathbf{H}_k^{\mathbf{T}} + \mathbf{R}_k]^{-\mathbf{1}}$
State Estimate Update	$\hat{\mathbf{x}}_k(+) = \hat{\mathbf{x}}_k(-) + \mathbf{K}_k[\mathbf{z}_k - \mathbf{H}_k\hat{\mathbf{x}}_k(-)]$
Error Covariance Update	$\mathbf{P}_k(+) = [\mathbf{I} - \mathbf{K}_k\mathbf{H}_k]\mathbf{P}_k(-)$
State Estimate Propagation	$\hat{\mathbf{x}}_{k+1}(-) = \mathbf{\Phi}_k\hat{\mathbf{x}}_k(+)$
Error Covariance Propagation	$\mathbf{P}_{k+1}(-) = \mathbf{\Phi}_k\mathbf{P}_k(+)\mathbf{\Phi}_k^{\mathbf{T}} + \mathbf{Q}_k$

4.2 The complementary Kalman filter for baseline vector estimation

The attitude estimator can be designed as a special case of the feedback complementary Kalman filter, shown as in Fig. 4. Without an inertial sensor to provide a reference trajectory, the process dynamics of the baseline vector states do not represent random sensor errors but rather "total" observer dynamics. When using the complementary configuration of Kalman filter for attitude estimation processing, attention should be paid on modelling the baseline vector kinematics. The baseline vector $\mathbf{b}$ can be calculated as the value at time $t = t_0$, plus a ramp function and a parabolic function. It can, therefore, be treated as taking the Taylor's series expansion for $\mathbf{b}$ about epoch *k*:

$$\mathbf{b}_{k+1} = \mathbf{b}_k + \dot{\mathbf{b}}_k \cdot \Delta t + \ddot{\mathbf{b}}_k \cdot \frac{\Delta t^2}{2} + \dddot{\mathbf{b}}_k \cdot \frac{\Delta t^3}{3} \cdots \tag{26}$$

The accurate description of the dynamics in the Kalman filter process model depends on the type of baseline vector (or platform/vehicle on which the antennas are attached) dynamics encountered in a given application, discussed as follows.

- *Stationary platform.* In the most basic form, the state vector should consist of three attitude states. The three-state filter, which includes three components of baseline vector in each of the three orthogonal directions, is ideal for a stationary receiver, where the random walk model is appropriate for the attitude states

$$\dot{\mathbf{b}} = \mathbf{u}_1(t) \tag{27}$$

where $\mathbf{u}_1(t) = [\mathrm{u}_x \quad \mathrm{u}_y \quad \mathrm{u}_z]^{\mathrm{T}}$ with strength (power spectral density, or simply PSD) $\mathbf{q}_1 = [q_x \quad q_y \quad q_z]^{\mathrm{T}}$ for the first-order model. The noise involved is a zero mean, Gaussian white noise process in each of the three orthogonal directions, and can be denoted as $\mathbf{u}_1(t) \sim N(0, \mathbf{q}_1)$. The associated discrete form for this process is

$$\mathbf{b}_{k+1} = \mathbf{b}_k + (\mathbf{w}_1)_k \tag{28}$$

As for the Kalman filter applications, a cure of unmodelled states induced divergence is to add additional 'fictitious' process noise to the system. The process noise has to be added to compensate for the unmodelled dynamics when ignoring the nonlinear terms. Therefore, it is necessary to select a sufficiently large $\mathbf{q}_1$ for the process noise to reflect the values of higher-order time derivative terms. Nevertheless, an appropriate (sufficiently large) $\mathbf{q}_1$ will help to catch the baseline vector dynamics, however, the solution accuracy may be decreased. Selection of a smaller $\mathbf{q}_1$ will result in a smoother output, with the risk that the baseline vector dynamics may be lost and filter divergence may occur.

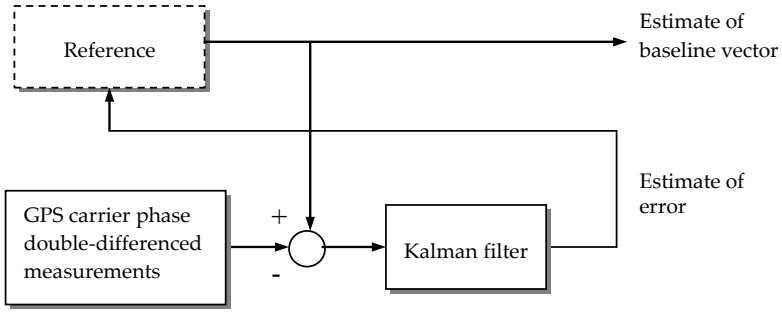

Figure 4: The complementary Kalman filter for baseline vector estimation

• *Low to medium dynamic platform.* If the baseline vector is moving nearly constant velocity, the model corresponding to the double integrator will be more suitable:

$$\ddot{\mathbf{b}} = \mathbf{u}_2(t),\ \mathbf{u}_2(t) \sim N(0, \mathbf{q}_2) \tag{29}$$

where the noise vector $\mathbf{u}_2 = [\mathrm{u}_{\ddot{x}} \quad \mathrm{u}_{\ddot{y}} \quad \mathrm{u}_{\ddot{z}}]^{\mathrm{T}}$, with the PSD vector $\mathbf{q}_2 = [q_{\ddot{x}} \quad q_{\ddot{y}} \quad q_{\ddot{z}}]^{\mathrm{T}}$ for the second-order model. The associated discrete form is

$$\mathbf{b}_{k+1} = \mathbf{b}_k + \dot{\mathbf{b}}_k \cdot \Delta t + (\mathbf{w}_2)_k$$

Selecting the state vector that contains the baseline vector position, $\mathbf{b}$, and the velocity, $\dot{\mathbf{b}}$.

$$\mathbf{x} \equiv \begin{bmatrix} \mathbf{b}_{3\times 1} \\ \dot{\mathbf{b}}_{3\times 1} \end{bmatrix}$$

the second-order filter model which possesses six states is then established

$$\frac{d}{dt}\begin{bmatrix} \mathbf{b}_{3\times 1} \\ \dot{\mathbf{b}}_{3\times 1} \end{bmatrix} = \begin{bmatrix} \mathbf{0}_{3\times 1} & \mathbf{I}_{3\times 1} \\ \mathbf{0}_{3\times 1} & \mathbf{0}_{3\times 1} \end{bmatrix}\begin{bmatrix} \mathbf{b}_{3\times 1} \\ \dot{\mathbf{b}}_{3\times 1} \end{bmatrix} + \begin{bmatrix} \mathbf{0}_{3\times 1} \\ \mathbf{u}_2 \end{bmatrix} \tag{30}$$

• *High dynamic platform.* When the baseline vector velocity cannot reasonably be modelled as constant, then acceleration states can be added.

$$\dddot{\mathbf{b}} = \mathbf{u}_3(t),\ \mathbf{u}_3(t) \sim N(0, \mathbf{q}_3) \tag{31}$$

where $\mathbf{u}_3 = [\mathrm{u}_{\dddot{x}} \quad \mathrm{u}_{\dddot{y}} \quad \mathrm{u}_{\dddot{z}}]^{\mathrm{T}}$, and $\mathbf{q}_3 = [q_{\dddot{x}} \quad q_{\dddot{y}} \quad q_{\dddot{z}}]^{\mathrm{T}}$ for the third-order model. The associated discrete form can be shown to be

$$\mathbf{b}_{k+1} = \mathbf{b}_k + \dot{\mathbf{b}}_k \cdot \Delta t + \ddot{\mathbf{b}}_k \cdot \frac{\Delta t^2}{2} + (\mathbf{w}_3)_k$$

In this case, the state vector contains the baseline vector position, $\mathbf{b}$, velocity, $\dot{\mathbf{b}}$, and acceleration, $\ddot{\mathbf{b}}$

$$\mathbf{x} \equiv \begin{bmatrix} \mathbf{b}_{3\times 1} & \dot{\mathbf{b}}_{3\times 1} & \ddot{\mathbf{b}}_{3\times 1} \end{bmatrix}^T$$

the resulting third-order filter model where nine states are involved, then becomes

$$\frac{d}{dt}\begin{bmatrix}\mathbf{b}_{3\times1}\\ \dot{\mathbf{b}}_{3\times1}\\ \ddot{\mathbf{b}}_{3\times1}\end{bmatrix}=\begin{bmatrix}\mathbf{0}_{3\times3} & \mathbf{I}_{3\times3} & \mathbf{0}_{3\times3}\\ \mathbf{0}_{3\times3} & \mathbf{0}_{3\times3} & \mathbf{I}_{3\times3}\\ \mathbf{0}_{3\times3} & \mathbf{0}_{3\times3} & \mathbf{0}_{3\times3}\end{bmatrix}\begin{bmatrix}\mathbf{b}_{3\times1}\\ \dot{\mathbf{b}}_{3\times1}\\ \ddot{\mathbf{b}}_{3\times1}\end{bmatrix}+\begin{bmatrix}\mathbf{0}_{3\times1}\\ \mathbf{0}_{3\times1}\\ \mathbf{u}_3\end{bmatrix} \tag{32}$$

With the double-differenced carrier phases as the measurements, it is seen that, when the second-order filter model is employed, the following relation holds:

$$\mathbf{z}=\begin{bmatrix}\nabla\Delta r_{12}^{12}\\ \nabla\Delta r_{12}^{13}\\ \vdots\\ \nabla\Delta r_{12}^{1n}\end{bmatrix}=\begin{bmatrix}(\mathbf{e}_1-\mathbf{e}_2)^{\mathrm{T}} & \mathbf{0}_{1\times3}\\ (\mathbf{e}_1-\mathbf{e}_3)^{\mathrm{T}} & \mathbf{0}_{1\times3}\\ \vdots & \vdots\\ (\mathbf{e}_1-\mathbf{e}_n)^{\mathrm{T}} & \mathbf{0}_{1\times3}\end{bmatrix}\begin{bmatrix}b_x\\ b_y\\ b_z\\ \dot{b}_x\\ \dot{b}_y\\ \dot{b}_z\end{bmatrix}+\mathbf{v}_k \tag{33}$$

It should be noted that, in the step of 'update estimate' in the flow chart, the parameter $\nabla\Delta\mathbf{r}_{k-measured}$ represents the double-differenced measurements from GPS satellites, while the predicted double-differenced measurements are

$$\nabla\Delta\hat{\mathbf{r}}_k(-)=\mathbf{H}_k\hat{\mathbf{b}}_k^e(-) \tag{34}$$

in which the measurement matrix for the second-order filter model is given by

$$\mathbf{H}_k=\begin{bmatrix}(\mathbf{e}_1-\mathbf{e}_2)^{\mathrm{T}} & \mathbf{0}_{1\times3}\\ (\mathbf{e}_1-\mathbf{e}_3)^{\mathrm{T}} & \mathbf{0}_{1\times3}\\ \vdots & \vdots\\ (\mathbf{e}_1-\mathbf{e}_n)^{\mathrm{T}} & \mathbf{0}_{1\times3}\end{bmatrix} \tag{35}$$

Based on the discussion above, the proposed algorithm for implementing the attitude determination is highlighted as follows:

1) Obtain the initial states (which include baseline vector and perhaps its time derivatives) and error covariance matrix.
2) Form the Kalman gain matrix.
3) Compute the predicted double-differenced measurements according to Eq. (34) to be shown later.
4) Update the state vector and error covariance matrix.
5) Propagate the state estimate to the next measurement epoch using the assumed model for the process dynamics.
6) Construct the rotation transformation matrix according to Eq. (15).
7) Determine the vehicle attitudes according to Eq. (14).

A flow chart is provided in Fig. 5 for implementation details.

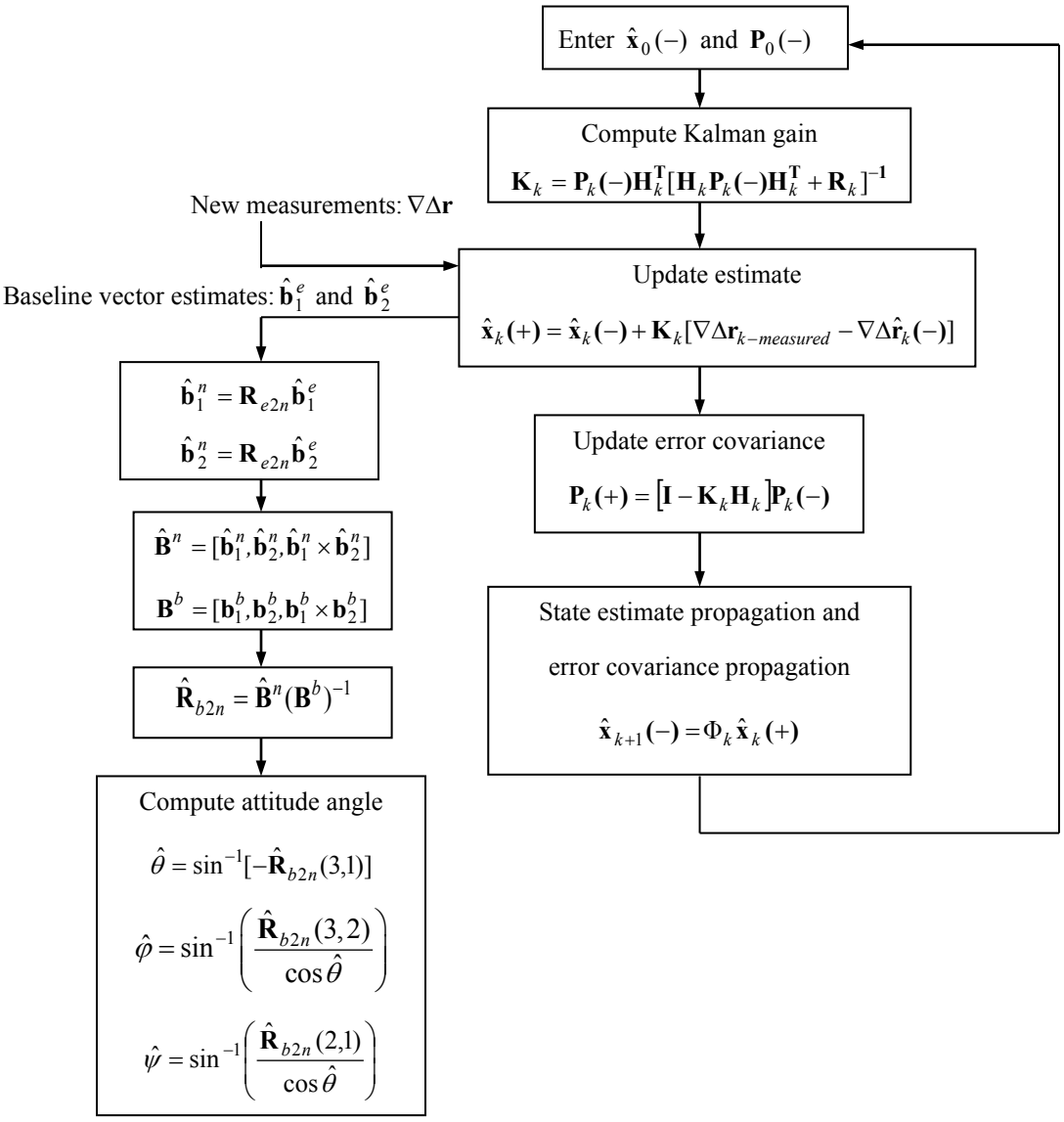

Figure 5: Flow chart of the proposed attitude determination mechanism

5 Illustrative examples

To validate the effectiveness of the proposed approach, simulation experiments have been carried out to evaluate the performance of the proposed approach in comparison with the other conventional methods for GPS-based attitude determination. Simulation was conducted for evaluating the filtering estimation performance of attitude solutions. The commercial software Satellite Navigation (SATNAV) Toolbox by GPSoft LLC [GPSoft LLC (2003)] was employed for generation of the GPS satellite orbits/positions and

thereafter, the satellite pseudoranges, carrier phase measurement, and constellation, required for simulation. The illustrative pseudorange error sources corrupting GPS measurements include ionospheric delay, tropospheric delay, receiver noise and multipath errors.

The antenna geometry is set up as that introduced in Section 3, with the baseline length variable d set to 1 meter and γ equal to 90 degrees. The attitude kinematics for simulation is assumed to be

$$\varphi(t) = 8\sin(\frac{\pi}{60}t)\ ;\ \theta(t) = 5\sin(\frac{\pi}{100}t)\ ;\ \psi(t) = 0.02t + 3\sin(\frac{\pi}{200}t)$$

for the time-varying roll, pitch, and yaw attitude angles, respectively. For this simulation example, a second-order Kalman filter model is employed. The noise variances for the process and measurement models are

$$\mathbf{GQG}^{\mathrm{T}} = \begin{bmatrix} \mathbf{0}_{3\times 3} & \cdots & \cdots & \cdots \\ \vdots & 1e-4 & 0 & 0 \\ \vdots & 0 & 1e-4 & 0 \\ \vdots & 0 & 0 & 1e-4 \end{bmatrix};\ \mathbf{R}_k = 0.1\mathbf{I}_{n\times n}$$

where n is the number of double-differenced measurements. After the integer ambiguity has been resolved, the proposed method in which Kalman filtering is used provides the baseline vector estimate with much better accuracy than the conventional method in which the least-squares approach is utilized. To avoid the filter divergence, it should be noted that setting the process noise variance to zero is not acceptable, since it can be very detrimental to the filtering performance, especially if the vehicle is manoeuvring rapidly. As a result, when the system reaches steady-state condition, the steady-state gain won't become zero and, subsequently, the filter is able to follow the time-varying attitude dynamics. A small value is admissible in practical design. However, one still needs to find the good values that meet the specific design/mission requirement. Figs. 6 and 7 present the estimate of the three-dimensional baseline vectors $\mathbf{b}_1$ and $\mathbf{b}_2$, respectively. The estimation accuracy of the baseline vectors are essential and directly influence the resulting accuracy of attitude angles. To confirm the correctness of the solutions, the estimated lengths for the baseline vectors are examed for validation. The estimated lengths for the two baseline vectors are shown as in Fig. 8. The attitude solutions are shown in Fig. 9 and thereafter Tab. 2 summarizes the error statistic of attitude solutions for both methods. It can be seen that estimation accuracy by the proposed method are improved remarkably. Incorporating the Kalman filter could catch the attitude kinematics well and achieved improved accuracy.

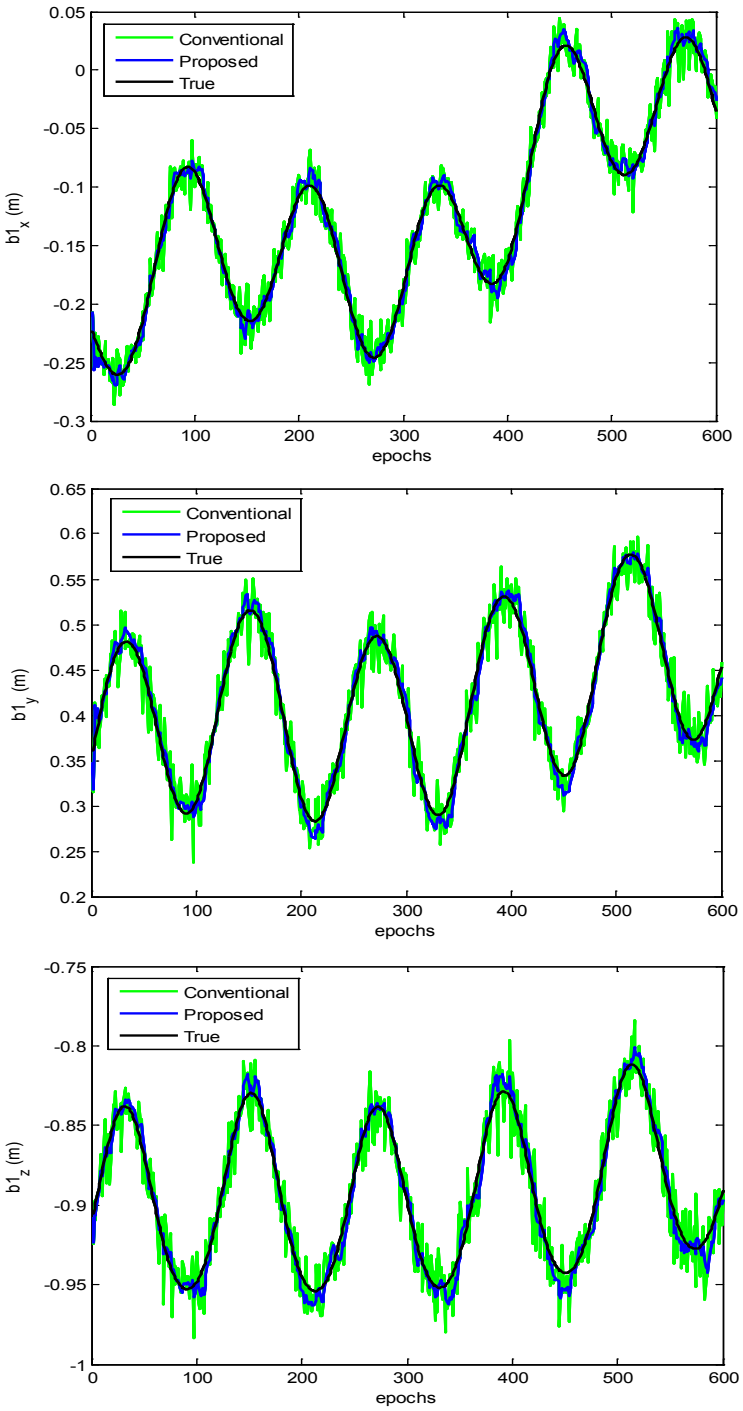

Figure 6: Estimate of the three-dimensional baseline vector $\mathbf{b}_1$

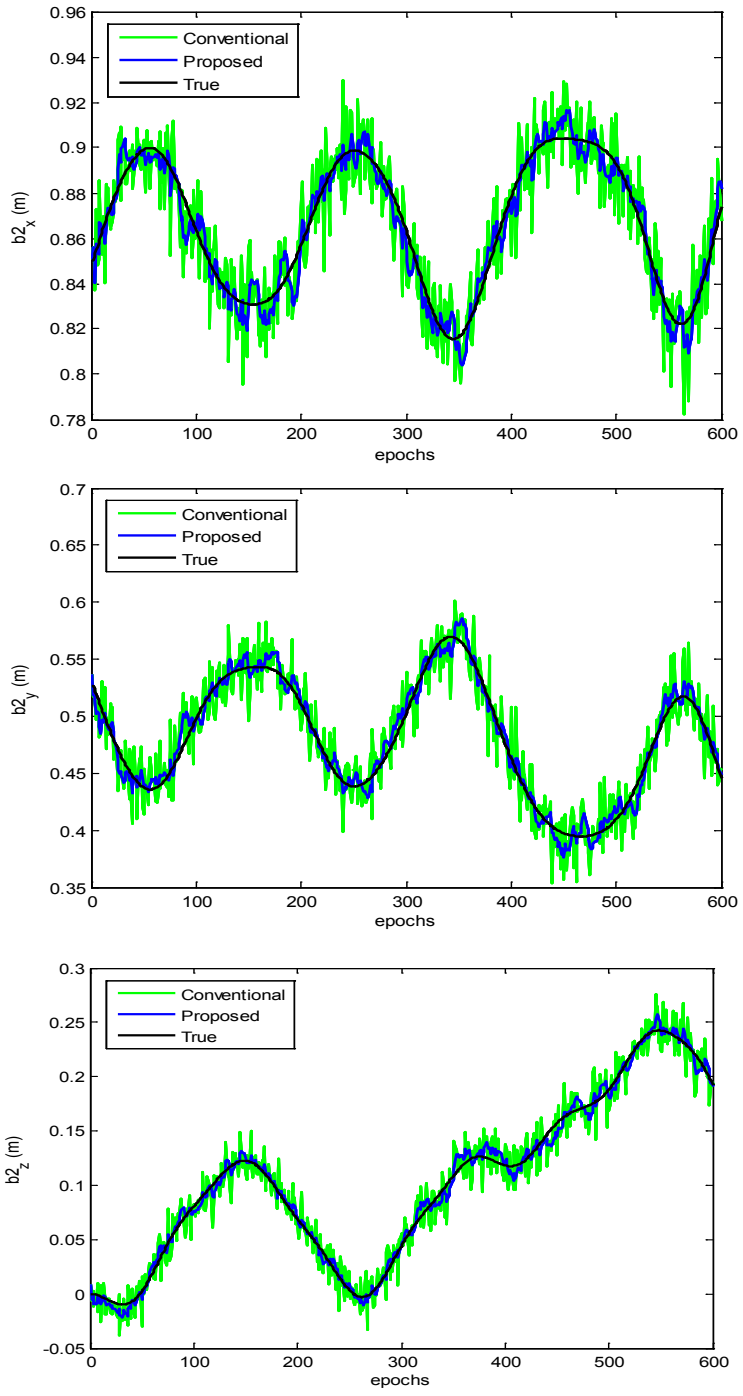

Figure 7: Estimate of the three-dimensional baseline vector $\mathbf{b}_2$

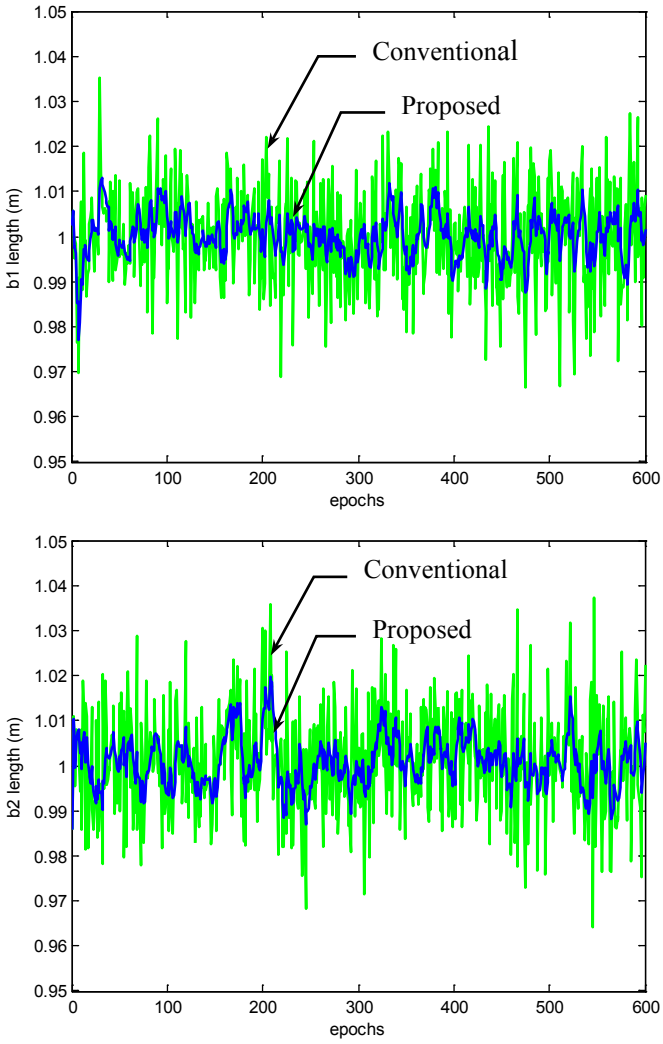

Figure 8: Estimate of the antenna baseline lengths: $\|\mathbf{b}_1\|$ and $\|\mathbf{b}_2\|$

Table 2: Error statistics for the attitude solutions

	Axis		**Roll**	**Pitch**	**Yaw**
Methods	Conventional	Mean (deg)	-0.0444	-0.0621	-0.0373
		Variance (deg^2)	1.7160	1.9520	0.4095
	Proposed	Mean (deg)	-0.0351	-0.0606	-0.0243
		Variance (deg^2)	0.4445	0.4248	0.0880

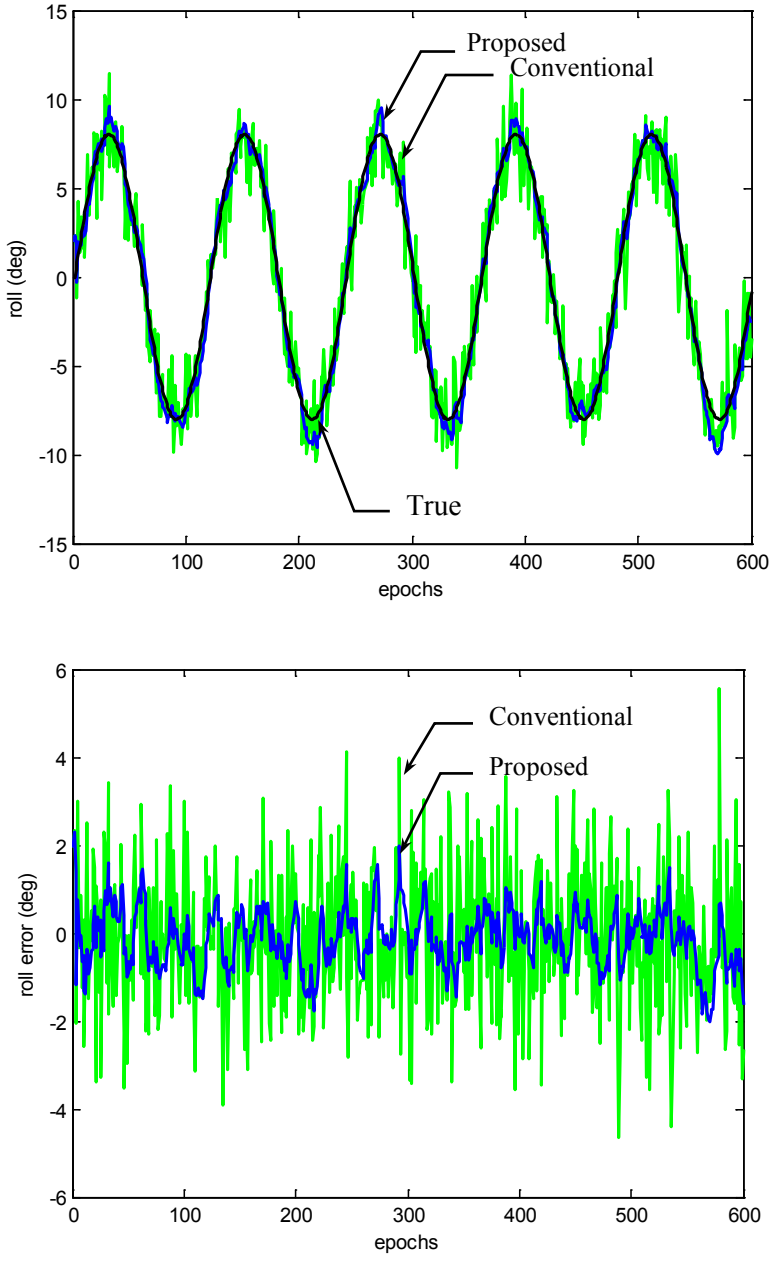
Proposed
Conventional
True
roll (deg)
epochs
Conventional
Proposed
roll error (deg)
epochs

(a) roll

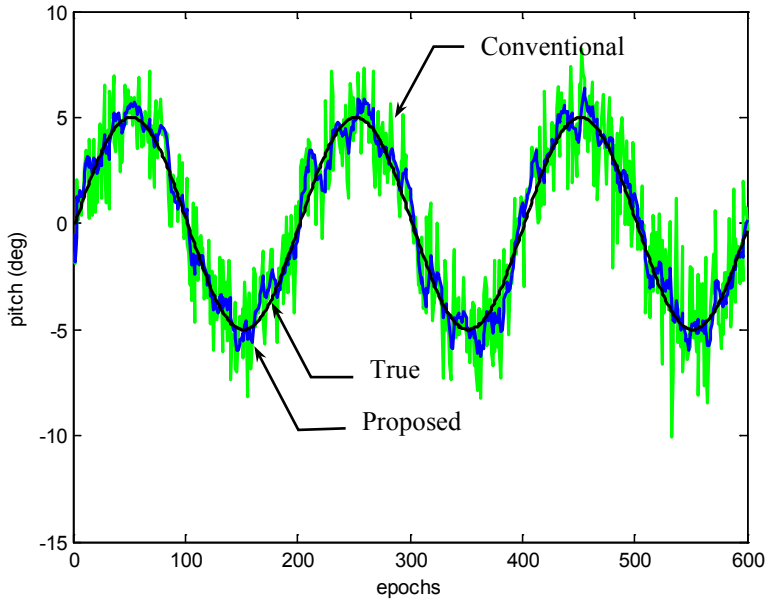
Conventional
True
Proposed
pitch (deg)
epochs
10
5
0
-5
-10
-15
0
100
200
300
400
500
600

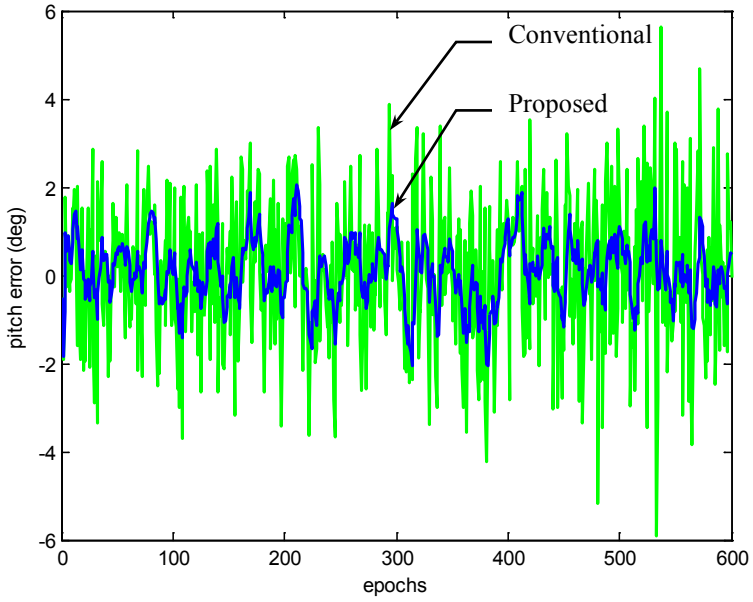
Conventional
Proposed
pitch error (deg)
epochs
6
4
2
0
-2
-4
-6
0
100
200
300
400
500
600

(b) pitch

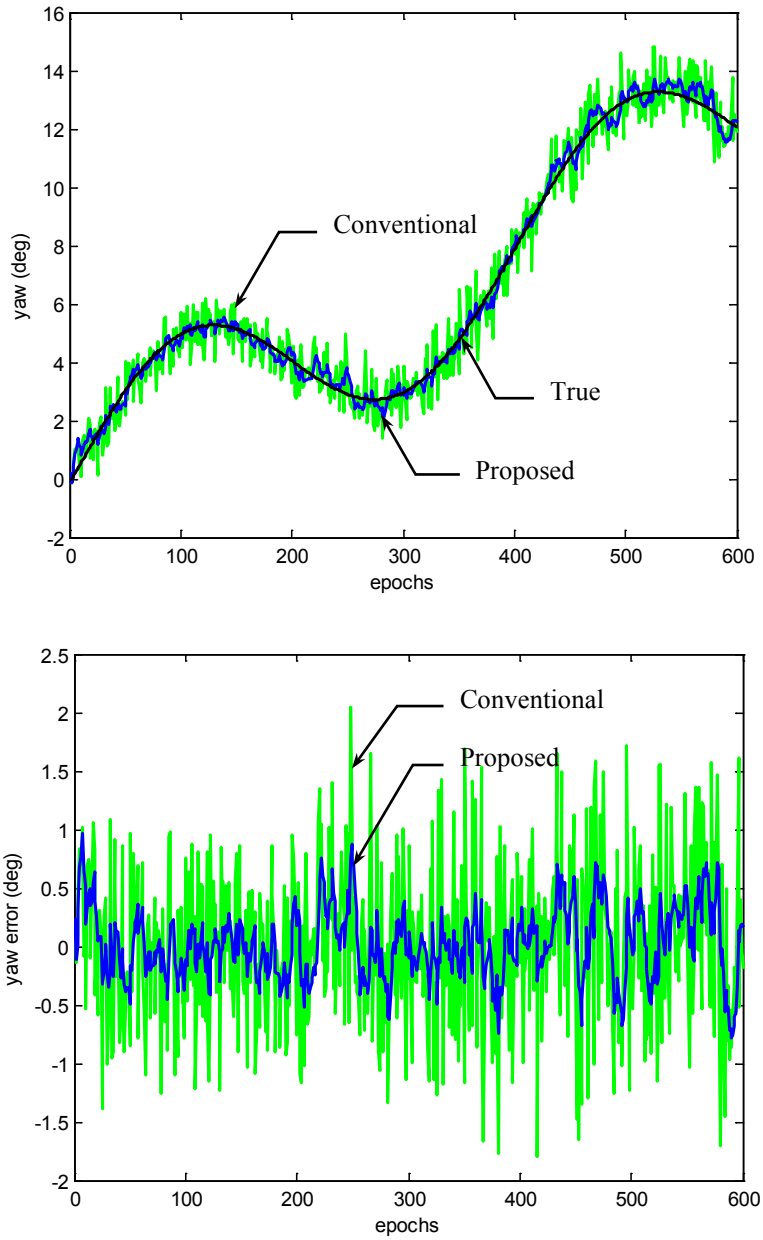

(c) yaw

Figure 9: Estimate of attitude angles and errors: (a) roll; (b) pitch; (c) yaw

6 Conclusions

The conventional attitude solutions provided by the interferometry technique are inherently noisy. This is due to the fact that, when the least-squares approach is employed, the estimate of baseline vectors based on the noisy double-differenced measurements will

be also inherently noisy. One way to improve the attitude solutions can be achieved by using the Kalman filter for estimating the baseline vectors. Details on implementing the proposed algorithms have been provided. Numerical simulations by employing a second order Kalman filter have been carried out. Results show that, by incorporating the Kalman filter into the GPS interferometer, noise errors in baseline vector solutions has been remarkably mitigated and therefore the estimation accuracy of the attitude solutions has been significantly improved.

In the example given in this paper, both the process and measurement noise parameters remained constant based on the assumption of stationary case. In the cases of high dynamic or multipath contaminated environment, the parameters in the two models need to be adequately tuned. Multipath is known as one of the dominant error sources in high accuracy satellite navigation systems. The multipath errors are among uncorrelated errors that are not cancelled out during observation differencing. When implementing the Kalman filter approach, poor knowledge of the noise statistics may seriously degrade the etimation performance, and even provoke the filter divergence. Further investigation can be carried on using the adaptive Kalman filter as the noise-adaptive filter for tuning the noise covariance matrices in the multipath environments.

Funding Statement: This work has been partially supported by the Ministry of Science and Technology of the Republic of China [Grant Number: MOST 108-2221-E-019-013].

Conflicts of Interest: The authors declare that they have no conflicts of interest to report regarding the present study.

References

Boccia, L; Amendola, G.; Di Massa, G. (2008): GNSS based attitude determination systems for high altitude platforms. *Satellite Communications and Navigation Systems*, pp. 199-210.

Brown, R. G.; Hwang, P. Y. C. (1997): *Introduction to Random Signals and Applied Kalman Filtering*. John Wiley & Sons, New York.

Chen, Y. T.; Wang, J.; Liu, S. J.; Chen, X.; Xiong, J. et al. (2019): Multiscale fast correlation filtering tracking algorithm based on a feature fusion model. *Concurrency and Computation: Practice and Experience*, e5533.

Chen, Y. T.; Xiong, J.; Xu, W. H.; Zuo, J. W. (2019): A novel online incremental and decremental learning algorithm based on variable support vector machine. *Cluster Computing*, vol. 22, no. 3, pp. 7435-7445.

Farrell J. A.; Barth, M. (1999): *The Global Positioning System & Inertial Navigation*. McCraw-Hill, New York.

Gelb, A. (1974): *Applied Optimal Estimation*. M. I. T. Press, MA.

GPSoft LLC (2003): *Satellite Navigation (SatNav) ToolBox 3.0 User's Guide*. Athens, Ohio.

Grewal M. S.; Andrews, A. P. (2001): *Kalman Filtering, Theory and Practice Using MATLAB*, 2nd Ed. John Wiley & Sons, Inc., New York.

Hauschild, A.; Montenbruck, O.; Langley, R. B. (2020): Flight results of GPS-based attitude determination for the Canadian CASSIOPE satellite. *Navigation*, vol. 67, no. 1, pp. 83-93.

Hofmann-Wellenhof, B.; Lichtenegger, H.; Wasle, E. (2008): *GNSS-Global Navigation Satellite Systems, GPS, GLONASS, Galileo, and More*. Springer Wien, New York.

Jwo D. J.; Cho, T. S. (2007): A practical note on evaluating Kalman filter performance optimality and degradation. *Applied Mathematics and Computation*, vol. 193, no. 2, pp. 482-505.

Kayton, M.; Fried, W. R. (1997): *Avionics Navigation Systems*. John Wiley & Sons.

Lewis, F. L. (1986): *Optimal Estimation*. John Wiley & Sons, Inc.

Li, H.; Nie, G.; Chen, D.; Wu, S.; Wang, K. (2019): Constrained MLAMBDA method for multi-GNSS structural health monitoring. *Sensors*, vol. 19, no. 20, pp. 4462.

Li, Y.; Efatmaneshnik, M.; Dempster, A. G. (2012): Attitude determination by integration of MEMS inertial sensors and GPS for autonomous agriculture applications. *GPS Solutions*, vol. 16, pp. 41-52.

Lu, L.; Ma, L.; Wu, T.; Chen, X. (2019): Performance analysis of positioning solution using low-cost single-frequency u-blox receiver based on baseline length constraint. *Sensors*, vol. 19, no. 19, pp. 4352.

Parkinson, B. W.; Spilker, J.; Axelrad, P.; Enge, P. (1996): *Global Positioning System: Theory and Applications*. American Institute of Aeronautics and Astronautics, Inc., Washington, DC.

Raskaliyev, A; Hosi Patel, S.; Sobh, T. M.; Ibrayev, A. (2020): GNSS-based attitude determination techniques-a comprehensive literature survey. *IEEE Access*, vol. 8, pp. 24873-24886.

Ryzhkov, L. M. (2019): Using GPS for attitude determination. *IEEE 5th International Conference Actual Problems of Unmanned Aerial Vehicles Developments*, pp. 199-201.

Van Grass, F.; Braasch, M. (1991-1992): GPS Interferometric attitude and heading determination: initial flight test results. *Navigation*, vol. 38, no. 4, pp. 359-378.

Wang, Q.; Yang, C.; Wu, S.; Wang, Y. (2019): Lever arm compensation of autonomous underwater vehicle for fast transfer alignment. *Computers, Materials & Continua*, vol. 59, no. 1, pp. 105-118.

Yin, C. Y.; Shi, L. F.; Sun, R. X; Wang, J. (2019): Improved collaborative filtering recommendation algorithm based on differential privacy protection. *Journal of Supercomputing*. https://doi.org/10.1007/s11227-019-02751-7.

Zhang, P.; Zhao, Y.; Lin, H.; Zou, J.; Wang, X. et al. (2020): A novel GNSS attitude determination method based on primary baseline switching for a multi-antenna platform. *Remote Sensing*, vol. 12, no. 5, pp. 747.